Journal of the Operations Research Society of Japan
Vol. 56, No. 2, June 2013, pp. 69–91

BLOCK-LEVEL SUCCESS AND LOSS RUNS FOR STREAMING SERVICES OVER WIRED-WIRELESS NETWORKS

Kota Kato
Kyoto University

Hiroyuki Masuyama
Kyoto University

Shoji Kasahara
Nara Institute of Science and Technology

Yutaka Takahashi
Kyoto University

(Received August 11, 2011; Revised December 17, 2012)

Abstract This paper considers the characteristics of block-level success and loss runs for streaming services over wired-wireless networks in which forward error correction (FEC) is employed for packet-loss resilience. We develop a single-server queueing model where the packet-transmission process over a wireless link is modeled by a Markovian service process (MSP) with two states "Good" and "Bad". The queueing system has two input processes: a general renewal input process and a Poisson one. The former represents a streaming-packet flow, while the latter is for background traffic multiplexed at the queue. We investigate the dynamics of the system state during the interval from the arrival epoch of the first packet of the block to that of the last one, deriving the block-loss (resp. block-success) run distribution, i.e., the probability distribution of the number of consecutive block loss (resp. success). The analytical model is validated by trace-driven simulation experiments. Numerical examples show that when the traffic intensity is high, the moments of block-level loss and success runs are significantly affected by the volume of background traffic and the FEC redundancy, rather than the system capacity.

Keywords: Queue, block-loss run, block-success run, forward error correction, GI+M/MSP/1/K queue

1. Introduction

With the recent advancement of broadband-network technologies, video streaming services has become one of the most popular applications over the Internet. Because video-streaming quality perceived by users is significantly affected by packet loss and delay, much effort has been devoted to how to prevent video-streaming packets from suffering packet loss and delay.

In terms of packet-loss resilience, forward error correction (FEC) is a well-known coding-based error recovery scheme. In this paper, we focus on packet-level FEC scheme [21]. In FEC, a sender host generates redundant data packets from original data ones, transmitting both original and redundant data packets to a receiver host. In the following, we assume that the sender host generates N redundant-data packets from D original-data packets. If the number of lost packets in a block is less than or equal to N, the receiver host can retrieve the original-data block. If more than N packets are lost, on the other hand, the block cannot be retrieved and lost. We call it a block loss hereafter. In general, block loss degrades quality of service (QoS) at application level, and hence it is important to investigate FEC recovery performance at application level.

The performance of FEC recovery has been extensively studied in the literature. Most of previous studies focused mainly on the block-loss probability. In general, however, the block-loss probability is not enough to evaluate the degradation of application-level QoS.

For example, consider a video streaming service over the Internet, in which a scalable video coding scheme like JPEG-2000 [16] or H.264 SVC [15] is employed with video traffic smoothing technique such as optimal smoothing [20]. In this case, the frame sizes can be set to a constant, and the resulting number of packets within a frame is also constant. Here, a video frame corresponds to a block of packets. Suppose that one hundred frames are sent to a destination terminal. Consider the following two block-loss scenarios. (1) For $1 \leq n \leq 10$, the nth frame, $(10+n)$th frame, $(20+n)$th frame, ..., and $(90+n)$th frame are lost. (2) For $1 \leq n \leq 91$, nth to $(n+9)$th frames are lost. Note that in both the cases, the block-loss probability is 0.1. From the application-level QoS point of view, however, the resultant video QoS in case (2) is worse than that in case (1). To the best of the authors' knowledge, the block-loss run distribution has not been fully studied yet.

Recent development of optical networking technology such as wavelength division multiplexing (WDM) results in that access networks are likely to be bottlenecks for data transmission (last mile bandwidth bottleneck [9]). On the other hand, wireless mesh networks (WMNs) including worldwide interoperability for microwave access (WiMAX) are expected to be a solution for the last mile issue for access networks [1]. In this paper, we focus on video streaming services over wired-wireless networks composed of optical backbone networks and wireless access ones. A video streaming server is placed on a backbone network, and a client node is connected to a wireless base station by a wireless link. Note here that the wireless base station is likely to be the bottleneck of data transmission for video streaming service due to interference and user mobility.

In this paper, we consider block-loss and block-success run events at the wireless base station. Here, the base station is modeled as a single-server queue with two independent arrival inputs, where a video-packet flow follows a general renewal input process and the packet-arrival process of background traffic is a Poisson one. The packet transmission process over a wireless link follows a Markovian service process with two states: "Good" and "Bad". If the wireless link is in Good (resp. Bad) state, the packet transmission rate is large (resp. small). The sojourn time of each state follows an exponential distribution. We analyze the block-loss and block-success run distributions, investigating how the block-loss and block-success runs are affected by the volume of background traffic, the FEC redundancy, the system size, the service rate, and the periods of alternating states.

The rest of this paper is organized as follows: Section 2 gives an overview of related work on the performance analysis of FEC recovery and packet-level loss and success runs. Section 3 describes our theoretical model. The theoretical model is analyzed in Section 4, and Section 5 shows numerical examples. Finally, Section 6 provides some conclusions.

2. Related Work

The effect of FEC redundancy on block-recovery performance has been extensively studied in the literature. In [6], Cidon et al. analyzed the distribution of the number of lost packets within a block of packets using an M/M/1/K queue. The effect of FEC redundancy on the block-loss probability was analyzed in [3] with an M/M/1/K queue. In these studies, however, a single-flow case was considered, and multiple-flow cases were not taken into consideration.

There is also much literature on the FEC recovery performance for switches and routers at which multiple input flows are superposed. Kawahara et al. considered a discrete-time finite-buffer queueing system with two input flows, in which the arrival process of main traffic including FEC is modeled as an interrupted Bernoulli process, while packets of background

traffic arrive at the system according to a Markov modulated Bernoulli process [13]. In [10], Hellal et al. considered a finite-buffer single-server queueing system with several independent Poisson arrival processes, analyzing the distribution of the number of lost packets within a block of packets. In [7, 8], Dán et al. analyzed the performance of FEC recovery using a finite-buffer single-server queueing system with two arrival processes. In [7], main traffic is assumed to be a Markov modulated Poisson process (MMPP), and background traffic a Poisson process. Furthermore, in [8], the packet flow of background traffic is also assumed to be an MMPP. In [17], Muraoka et al. considered the FEC recovery performance with a GI+M/M/1/K queue, deriving the packet- and block-loss probabilities. In [18], the authors extended the analytical model of [17] to the one where the packet-transmission time is governed by a Markovian service process (MSP). Note that all the studies mentioned above paid no attention to block-loss run events.

In terms of block-level success and loss run events, Jiang and Schulzrinne [11] proposed the use of the extended Gilbert model, and the inter-loss distance, which is equivalent to packet-success run, was studied for describing the temporal dependence of packet loss. Yajnik et al. [24] statistically analyzed packet-loss and packet-success runs using trace data obtained from end-to-end measurements of unicast and multicast Internet connections. They showed that packet-loss run lengths and packet-success run lengths are geometrically distributed in many cases. They also modeled the data with three models: the Bernoulli model, the two-state Markov chain model, and the kth order Markov chain model. Note that in these works, the authors considered packet-level loss and success run lengths.

In our previous work [12], we considered the block-loss run event at a bottleneck router in a backbone network. Here, the bottleneck router is modeled as a GI+M/M/1/K queue, where a video packet flow follows a general renewal input process and the packet-arrival process of background traffic is a Poisson one. We analyzed the block-loss run distribution and investigated how the block-loss run is affected by the volume of background traffic, the FEC redundancy, and the system size. In this paper, we extend the analytical model of [12] to the case where the packet-transmission process of a wireless link in a wired-wireless network is governed by an MSP. We consider not only block-level loss run but also block-level success run.

3. Analytical Model

3.1. Target of modeling

We consider the situation in which packets of a video stream are transferred from a sender host to a receiver host over wired-wireless networks. Suppose that a wireless base station is in congestion. The video packets do not suffer from packet loss at any routers except the wireless base station. In the base station, not only video packets but also packets transmitted by other hosts are multiplexed. In the following, the video-packet flow is referred to as main traffic, and the packets from the other hosts as background traffic. (See Figure 1. In this figure, solid arrows indicate wired links, while dashed arrows represent wireless links.)

3.2. Analytical model

We model the wireless base station by an FCFS single-server queue with two independent arrival processes and a single finite buffer. The buffer size of the wireless base station is equal to $K-1$ ($K \geq 1$), that is, the total capacity of the system is equal to K. Packets of main traffic arrive at the wireless base station in sequence, and its inter-arrival times are independent and identically distributed (i.i.d.) with a general distribution $G(x)$ ($x \geq 0$). Furthermore, packets of background traffic form a Poisson arrival process with rate λ.

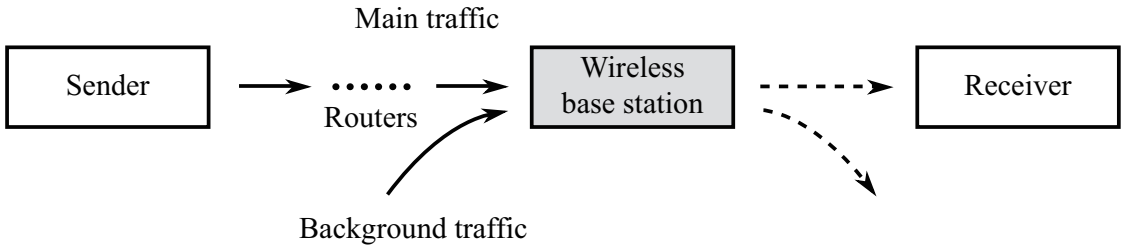

Figure 1: Wireless base station

The packet transmission times for both main and background traffic follow an MSP with two states "Good" and "Bad", which was originally developed in [5]. The wireless link is regarded as in Bad state when the signal power is below a given threshold. When the signal power is greater than or equal to the threshold, on the other hand, the wireless link is modeled as in Good state. Note that when the wireless link is in Bad state, link-level error is likely to occur, resulting in packet loss. We assume that link-level error is concealed by retransmission mechanism such as automatic-repeat request (ARQ), and hence no packet loss occurs at the wireless link. Note also that error recovery by retransmission increases the packet-transmission time*. In the following, we denote "Good" and "Bad" by "G" and "B", respectively. The lengths of states G and B are i.i.d. according to exponential distributions with mean $1/\alpha$ and $1/\beta$, respectively. While being in state G (resp. B), a service rate of a packet is equal to μ_G (resp. μ_B)†. From the assumption of retransmission mechanism, we have $\mu_G > \mu_B$. When an arriving packet finds K packets in the system, the packet is dropped and lost.

We assume that a video frame consists of D data packets, from which N redundant packets are generated. Then the D data packets and N redundant packets are aggregated to a *block*. Thus a block contains $M \triangleq D + N$ packets. If the number of lost packets in a block is less than N, the original data of the block are recovered through FEC decoding at the receiver host. Otherwise the receiver host cannot recover the original data, resulting in a loss of the block.

4. Analysis

We first discuss, in subsection 4.1, the stationary joint distribution of the number of packets in the wireless base station and the state of service immediately before a packet arrival in main traffic. Next we consider the counting process of lost packets in main traffic in subsection 4.2. Based on these results, we derive the limit distribution of the block-loss and block-success runs in subsection 4.3.

*It is shown in [4] that when Stop-and-Wait ARQ is assumed, the packet-transmission time including retransmission times can be modeled by geometric distribution with the packet loss probability p. In this case, the mean packet-transmission time including retransmission times due to packet loss is proportional to $1/(1-p)$. This implies that the packet-transmission rate decreases with the increase in the packet-loss probability. See [4] for details.

†The measurement-based analysis in [2] shows that link delays over a wireless mesh network are well fitted by gamma or logistic distributions. In [22], the effect of retransmission mechanism on the packet transmission time is considered. It is shown in [22] that the packet transmission time for a communication link governed by an ON-OFF process has an exponential tail under certain conditions. Those studies suggest that the packet transmission time over a wireless link can be modeled by an exponential distribution.

4.1. Joint distribution of queue-length and server-state

Let $L(t)$ $(t \geq 0)$ denote the number of packets in the wireless base station at time t. Let $S(t)$ $(t \geq 0)$ denote the state of service. We assume that $\{L(t)\}$ and $\{S(t)\}$ are right-continuous and have left-hand limits. We also assume that in main traffic, packets arrive at times $0 = T_1 < T_2 < T_3 < \cdots$. Let L_k, L_k^-, S_k and S_k^- denote

$$\begin{aligned} L_k &= L(T_k), \qquad L_k^- = L(T_k-), \\ S_k &= S(T_k), \qquad S_k^- = S(T_k-), \end{aligned}$$

respectively. Clearly, $L_k = \min(L_k^- + 1, K)$ $(k = 1, 2, \ldots)$, and $S_k = S_k^-$ $(k = 1, 2, \ldots)$ with probability one. Let $(j, s)_m$ and $(j, s)_m^-$ denote events $\{L_m = j,\ S_m = s\}$ and $\{L_m^- = j,\ S_m^- = s\}$, respectively. We then define $\mathbf{\Gamma}^{+-}$ and $\mathbf{\Pi}^{--}$ as $2(K+1) \times 2(K+1)$ matrices such that

$$\mathbf{\Gamma}^{+-} = \begin{pmatrix} \mathbf{\Gamma}_{0,0}^{+-} & \mathbf{\Gamma}_{0,1}^{+-} & \cdots & \mathbf{\Gamma}_{0,K}^{+-} \\ \mathbf{\Gamma}_{1,0}^{+-} & \mathbf{\Gamma}_{1,1}^{+-} & \cdots & \mathbf{\Gamma}_{1,K}^{+-} \\ \vdots & \vdots & \ddots & \vdots \\ \mathbf{\Gamma}_{K,0}^{+-} & \mathbf{\Gamma}_{K,1}^{+-} & \cdots & \mathbf{\Gamma}_{K,K}^{+-} \end{pmatrix},$$

$$\mathbf{\Pi}^{--} = \begin{pmatrix} \mathbf{\Pi}_{0,0}^{--} & \mathbf{\Pi}_{0,1}^{--} & \cdots & \mathbf{\Pi}_{0,K}^{--} \\ \mathbf{\Pi}_{1,0}^{--} & \mathbf{\Pi}_{1,1}^{--} & \cdots & \mathbf{\Pi}_{1,K}^{--} \\ \vdots & \vdots & \ddots & \vdots \\ \mathbf{\Pi}_{K,0}^{--} & \mathbf{\Pi}_{K,1}^{--} & \cdots & \mathbf{\Pi}_{K,K}^{--} \end{pmatrix},$$

where

$$\mathbf{\Gamma}_{i,j}^{+-} = \begin{pmatrix} \Pr[(j,G)_{k+1}^- \mid (i,G)_k] & \Pr[(j,B)_{k+1}^- \mid (i,G)_k] \\ \Pr[(j,G)_{k+1}^- \mid (i,B)_k] & \Pr[(j,B)_{k+1}^- \mid (i,B)_k] \end{pmatrix},$$

$$\mathbf{\Pi}_{i,j}^{--} = \begin{pmatrix} \Pr[(j,G)_{k+1}^- \mid (i,G)_k^-] & \Pr[(j,B)_{k+1}^- \mid (i,G)_k^-] \\ \Pr[(j,G)_{k+1}^- \mid (i,B)_k^-] & \Pr[(j,B)_{k+1}^- \mid (i,B)_k^-] \end{pmatrix}.$$

It is easy to see that

$$\mathbf{\Pi}^{--} = \mathbf{\Lambda}^{-+}\mathbf{\Gamma}^{+-}, \tag{4.1}$$

where $\mathbf{\Lambda}^{-+}$ denotes a $2(K+1) \times 2(K+1)$ matrix such that

$$\mathbf{\Lambda}^{-+} = \begin{pmatrix} \boldsymbol{O} & \boldsymbol{I}_2 & \boldsymbol{O} & \cdots & \boldsymbol{O} & \boldsymbol{O} \\ \boldsymbol{O} & \boldsymbol{O} & \boldsymbol{I}_2 & \ddots & \boldsymbol{O} & \boldsymbol{O} \\ \vdots & \vdots & \ddots & \ddots & \vdots & \vdots \\ \boldsymbol{O} & \boldsymbol{O} & \boldsymbol{O} & \ddots & \boldsymbol{I}_2 & \boldsymbol{O} \\ \boldsymbol{O} & \boldsymbol{O} & \boldsymbol{O} & \cdots & \boldsymbol{O} & \boldsymbol{I}_2 \\ \boldsymbol{O} & \boldsymbol{O} & \boldsymbol{O} & \cdots & \boldsymbol{O} & \boldsymbol{I}_2 \end{pmatrix}. \tag{4.2}$$

Note here that $\boldsymbol{I}_2$ denotes the 2×2 identity matrix.

Recall that during time interval (T_k, T_{k+1}), no arrivals from main traffic occur whereas ones from background traffic follow a Poisson process with rate λ. Recall also that the service times of all packets both in main and background traffic are according to an MSP. These facts imply that during time interval (T_k, T_{k+1}), the behavior of $\{L(t), S(t)\}$ is stochastically

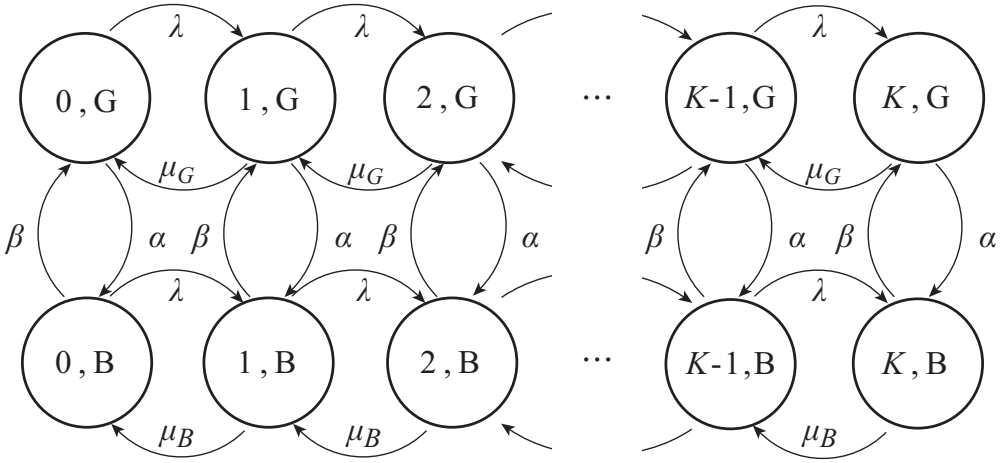

Figure 2: State transition diagram of $\{L(t), S(t)\}$

equivalent to that of the queue length process in an M/MSP/1/K queue, to be more specific, a continuous-time bivariate Markov chain driven by an infinitesimal generator $\boldsymbol{Q}$ such that

$$\boldsymbol{Q} = \begin{pmatrix} \underline{\boldsymbol{Q}}_0 & \boldsymbol{Q}_1 & \boldsymbol{O} & \cdots & \boldsymbol{O} & \boldsymbol{O} \\ \boldsymbol{Q}_{-1} & \boldsymbol{Q}_0 & \boldsymbol{Q}_1 & \ddots & \vdots & \vdots \\ \boldsymbol{O} & \boldsymbol{Q}_{-1} & \boldsymbol{Q}_0 & \ddots & \boldsymbol{O} & \boldsymbol{O} \\ \boldsymbol{O} & \boldsymbol{O} & \boldsymbol{Q}_{-1} & \ddots & \boldsymbol{Q}_1 & \boldsymbol{O} \\ \vdots & \vdots & \ddots & \ddots & \boldsymbol{Q}_0 & \boldsymbol{Q}_1 \\ \boldsymbol{O} & \boldsymbol{O} & \boldsymbol{O} & \ddots & \boldsymbol{Q}_{-1} & \overline{\boldsymbol{Q}}_0 \end{pmatrix},$$

where $\boldsymbol{Q}_{-1}$, $\boldsymbol{Q}_1$, $\boldsymbol{Q}_0$, $\underline{\boldsymbol{Q}}_0$, and $\overline{\boldsymbol{Q}}_0$ are defined as

$$\begin{aligned} \boldsymbol{Q}_{-1} &= \begin{pmatrix} \mu_G & 0 \\ 0 & \mu_B \end{pmatrix}, \quad \boldsymbol{Q}_1 = \lambda \boldsymbol{I}_2, \\ \boldsymbol{Q}_0 &= \begin{pmatrix} -(\alpha+\lambda+\mu_G) & \alpha \\ \beta & -(\beta+\lambda+\mu_B) \end{pmatrix}, \\ \underline{\boldsymbol{Q}}_0 &= \begin{pmatrix} -(\alpha+\lambda) & \alpha \\ \beta & -(\beta+\lambda) \end{pmatrix}, \\ \overline{\boldsymbol{Q}}_0 &= \begin{pmatrix} -(\alpha+\mu_G) & \alpha \\ \beta & -(\beta+\mu_B) \end{pmatrix}, \end{aligned}$$

respectively (see Figure 2). Thus we have

$$\boldsymbol{\Gamma}^{+-} = \int_0^\infty \exp(\boldsymbol{Q}x)\mathrm{d}G(x). \tag{4.3}$$

It follows from (4.2) and (4.3) that the transition probability matrix $\boldsymbol{\Pi}^{--}$ in (4.1) is irreducible and aperiodic and therefore ergodic due to the finiteness of the state space. As a result, $\boldsymbol{\Pi}^{--}$ has the unique stationary probability vector $\boldsymbol{\pi}^- = (\pi^-_{l,s}; l, s \in \{0, 1, \ldots, K\} \times \{G, B\})$, which satisfies

$$\pi^-_{l,s} = \lim_{k\to\infty} \Pr(L^-_k = l, S^-_k = s).$$

4.2. Counting process of lost packets in main traffic

We refer to the packet arriving at time T_m as packet m. Let θ_m denote a random variable that takes value 1 if packet m is lost; otherwise takes value 0. Let $N_m = \sum_{i=1}^{m} \theta_i$ for $m = 1, 2, \ldots$. We then consider the counting process $\{N_m; m = 1, 2, \ldots\}$ of lost packets in main traffic.

For each $m = 1, 2, \ldots$, let $\boldsymbol{P}_{m,i,j}^{-+}(k)$ $(k = 1, 2, \ldots, m,\ i, j = 0, 1, \ldots, K)$ denote 2×2 matrix such that

$$\begin{pmatrix} \Pr[(j,G,k)_m \mid (i,G)_1^-] & \Pr[(j,B,k)_m \mid (i,G)_1^-] \\ \Pr[(j,G,k)_m \mid (i,B)_1^-] & \Pr[(j,B,k)_m \mid (i,B)_1^-] \end{pmatrix},$$

where $(j, s, k)_m$ represents an event $\{L_m = j,\ S_m = s, N_m = k\}$. Further let $\widetilde{\boldsymbol{P}}_m^{-+}(z) = \sum_{k=0}^{m} z^k \boldsymbol{P}_m^{-+}(k)$, where $\boldsymbol{P}_m^{-+}(k)$ $(k = 1, 2, \ldots, m)$ denotes a $2(K+1) \times 2(K+1)$ matrix such that

$$\boldsymbol{P}_m^{-+}(k) = \begin{pmatrix} \boldsymbol{P}_{m,0,0}^{-+}(k) & \boldsymbol{P}_{m,0,1}^{-+}(k) & \cdots & \boldsymbol{P}_{m,0,K}^{-+}(k) \\ \boldsymbol{P}_{m,1,0}^{-+}(k) & \boldsymbol{P}_{m,1,1}^{-+}(k) & \cdots & \boldsymbol{P}_{m,1,K}^{-+}(k) \\ \vdots & \vdots & \ddots & \vdots \\ \boldsymbol{P}_{m,K,0}^{-+}(k) & \boldsymbol{P}_{m,K,1}^{-+}(k) & \cdots & \boldsymbol{P}_{m,K,K}^{-+}(k) \end{pmatrix}.$$

It then follows that

$$\begin{aligned} \widetilde{\boldsymbol{P}}_1^{-+}(z) &= \boldsymbol{P}_1^{-+}(0) + z\boldsymbol{P}_1^{-+}(1) \\ &= \begin{pmatrix} \boldsymbol{O} & \boldsymbol{I}_2 & \boldsymbol{O} & \cdots & \boldsymbol{O} \\ \boldsymbol{O} & \boldsymbol{O} & \boldsymbol{I}_2 & \ddots & \boldsymbol{O} \\ \vdots & \vdots & \ddots & \ddots & \vdots \\ \boldsymbol{O} & \boldsymbol{O} & \cdots & \boldsymbol{O} & \boldsymbol{I}_2 \\ \boldsymbol{O} & \boldsymbol{O} & \cdots & \boldsymbol{O} & \boldsymbol{O} \end{pmatrix} + z \begin{pmatrix} \boldsymbol{O} & \cdots & \boldsymbol{O} & \boldsymbol{O} \\ \vdots & \ddots & \vdots & \vdots \\ \boldsymbol{O} & \cdots & \boldsymbol{O} & \boldsymbol{O} \\ \boldsymbol{O} & \cdots & \boldsymbol{O} & \boldsymbol{I}_2 \end{pmatrix}. \end{aligned}$$

We next consider $\{\widetilde{\boldsymbol{P}}_m^{-+}(z); m = 2, 3, \ldots\}$. Let $\boldsymbol{A}_{i,j}^{++}(\theta)$ $(i, j = 0, 1, \ldots, K,\ \theta = 0, 1)$ denote

$$\begin{pmatrix} \Pr[(j,G,\theta)_m^A \mid (i,G)_{m-1}] & \Pr[(j,B,\theta)_m^A \mid (i,G)_{m-1}] \\ \Pr[(j,G,\theta)_m^A \mid (i,B)_{m-1}] & \Pr[(j,B,\theta)_m^A \mid (i,B)_{m-1}] \end{pmatrix},$$

where $(j, s, \theta)_m^A$ denotes an event $\{L_m = j,\ S_m = s, \theta_m = \theta\}$. Let $\boldsymbol{A}^{++}(\theta)$ denote a $2(K+1) \times 2(K+1)$ matrix such that

$$\boldsymbol{A}^{++}(\theta) = \begin{pmatrix} \boldsymbol{A}_{0,0}^{++}(\theta) & \boldsymbol{A}_{0,1}^{++}(\theta) & \cdots & \boldsymbol{A}_{0,K}^{++}(\theta) \\ \boldsymbol{A}_{1,0}^{++}(\theta) & \boldsymbol{A}_{1,1}^{++}(\theta) & \cdots & \boldsymbol{A}_{1,K}^{++}(\theta) \\ \vdots & \vdots & \ddots & \vdots \\ \boldsymbol{A}_{K,0}^{++}(\theta) & \boldsymbol{A}_{K,1}^{++}(\theta) & \cdots & \boldsymbol{A}_{K,K}^{++}(\theta) \end{pmatrix}.$$

Note here that the event $\{\theta_m = 0\}$ is equivalent to the event $\{0 \le L_m^- \le K - 1\}$ whereas

the event $\{\theta_m = 1\}$ is equivalent to the event $\{L_m^- = K\}$. It thus follows that

$$\boldsymbol{A}^{++}(0) = \begin{pmatrix} \boldsymbol{O} & \boldsymbol{O} & \boldsymbol{O} & \cdots & \boldsymbol{O} \\ \boldsymbol{O} & \boldsymbol{\Gamma}_{1,0}^{+-} & \boldsymbol{\Gamma}_{1,1}^{+-} & \cdots & \boldsymbol{\Gamma}_{1,K-1}^{+-} \\ \boldsymbol{O} & \boldsymbol{\Gamma}_{2,0}^{+-} & \boldsymbol{\Gamma}_{2,1}^{+-} & \cdots & \boldsymbol{\Gamma}_{2,K-1}^{+-} \\ \vdots & \vdots & \vdots & \ddots & \vdots \\ \boldsymbol{O} & \boldsymbol{\Gamma}_{K,0}^{+-} & \boldsymbol{\Gamma}_{K,1}^{+-} & \cdots & \boldsymbol{\Gamma}_{K,K-1}^{+-} \end{pmatrix},$$

$$\boldsymbol{A}^{++}(1) = \begin{pmatrix} \boldsymbol{O} & \cdots & \boldsymbol{O} & \boldsymbol{O} \\ \boldsymbol{O} & \cdots & \boldsymbol{O} & \boldsymbol{\Gamma}_{1,K}^{+-} \\ \boldsymbol{O} & \cdots & \boldsymbol{O} & \boldsymbol{\Gamma}_{2,K}^{+-} \\ \vdots & \ddots & \vdots & \vdots \\ \boldsymbol{O} & \cdots & \boldsymbol{O} & \boldsymbol{\Gamma}_{K,K}^{+-} \end{pmatrix}.$$

By definition, we have for $m = 2, 3, \ldots,$

$$\widetilde{\boldsymbol{P}}_m^{-+}(z) = \widetilde{\boldsymbol{P}}_{m-1}^{-+}(z)(\boldsymbol{A}^{++}(0) + z\boldsymbol{A}^{++}(1)). \tag{4.4}$$

Therefore from (4.4), we obtain the recursion for $\{\boldsymbol{P}_m^{-+}(k)\}$: for $m = 2, 3, \ldots,$

$$\boldsymbol{P}_m^{-+}(0) = \boldsymbol{P}_{m-1}^{-+}(0)\boldsymbol{A}^{++}(0), \tag{4.5}$$

and for $k = 1, 2, \ldots, M,$

$$\boldsymbol{P}_m^{-+}(k) = \boldsymbol{P}_{m-1}^{-+}(k-1)\boldsymbol{A}^{++}(1) + \boldsymbol{P}_{m-1}^{-+}(k)\boldsymbol{A}^{++}(0). \tag{4.6}$$

4.3. Limit distributions of the block-loss and block-success runs

We assume that the head packet of a block arrives at time $T_1 = 0$ and the subsequent $M-1$ packets of the block arrive at time $T_2 < T_3 < \cdots < T_M$. We refer to the block arriving at time 0 as block 1 and the subsequent blocks as block 2, block 3,.... We then assume that block n ($n = 1, 2, \ldots$) consists of packets $(n-1)M + 1$ through nM, which implies that the head packet of block n arrives at time $\widehat{T}_n \triangleq T_{(n-1)M+1}$. Let $\widehat{L}_n^- = L(\widehat{T}_n-)$ and $\widehat{S}_n^- = S(\widehat{T}_n-)$.

In what follows, we consider the limit distributions of the block-loss and block-success run. For simplicity and to save space, we denote $\Pr[\,\cdot \mid \widehat{L}_1^-(= L_1^-) = \gamma]$ by $\mathbb{P}_\gamma[\,\cdot\,]$ and the set of positive integers by $\mathbb{N}$. Let Θ_ν ($\nu \in \mathbb{N}$) denote a random variable such that $\Theta_\nu = 1$ if block ν is lost; and otherwise $\Theta_\nu = 0$. Let

$$\begin{aligned} X_{\mathrm{BL}}^{(\nu)} &= \inf\{n \in \mathbb{N}; \Theta_{\nu+n+1} = 0 \mid (\Theta_\nu, \Theta_{\nu+1}) = (0,1)\}, \\ X_{\mathrm{BS}}^{(\nu)} &= \inf\{n \in \mathbb{N}; \Theta_{\nu+n+1} = 1 \mid (\Theta_\nu, \Theta_{\nu+1}) = (1,0)\}, \end{aligned}$$

which are called *block-loss run length* and *block-success run length*, respectively. For any fixed $\gamma = 0, 1, \ldots, K$, we define $P_{\mathrm{BL}}(n)$ and $P_{\mathrm{BS}}(n)$ ($n \in \mathbb{N}$) as

$$\begin{aligned} P_{\mathrm{BL}}(n) &= \lim_{\nu\to\infty} \mathbb{P}_\gamma[X_{\mathrm{BL}}^{(\nu)} = n \mid (\Theta_\nu, \Theta_{\nu+1}) = (0,1)] \\ &= \lim_{\nu\to\infty} \frac{\mathbb{P}_\gamma[(\Theta_\nu, \Theta_{\nu+1}, \ldots, \Theta_{\nu+n}, \Theta_{\nu+n+1}) = (0,1,\ldots,1,0)]}{\mathbb{P}_\gamma[(\Theta_\nu, \Theta_{\nu+1}) = (0,1)]}, \qquad (4.7) \\ P_{\mathrm{BS}}(n) &= \lim_{\nu\to\infty} \mathbb{P}_\gamma[X_{\mathrm{BS}}^{(\nu)} = n \mid (\Theta_\nu, \Theta_{\nu+1}) = (1,0)] \\ &= \lim_{\nu\to\infty} \frac{\mathbb{P}_\gamma[(\Theta_\nu, \Theta_{\nu+1}, \ldots, \Theta_{\nu+n}, \Theta_{\nu+n+1}) = (1,0,\ldots,0,1)]}{\mathbb{P}_\gamma[(\Theta_\nu, \Theta_{\nu+1}) = (1,0)]}, \qquad (4.8) \end{aligned}$$

respectively. We also define X_{BL} and X_{BS} as random variables such that $\Pr[X_{\mathrm{BL}} = n] = P_{\mathrm{BL}}(n)$ and $\Pr[X_{\mathrm{BS}} = n] = P_{\mathrm{BS}}(n)$, respectively, for $n \in \mathbb{N}$. Then X_{BL} and X_{BS} can be considered as generic random variables for the block-loss run and block-success run, respectively, in steady state.

Let $\boldsymbol{R}_{i,j}$ and $\boldsymbol{S}_{i,j}$ denote 2×2 matrices such that

$$\begin{aligned}
\boldsymbol{R}_{i,j} &= \begin{pmatrix} \Pr[\langle j, G, 1\rangle^-_{\nu+1} \mid \langle i, G\rangle^-_{\nu}] & \Pr[\langle j, B, 1\rangle^-_{\nu+1} \mid \langle i, G\rangle^-_{\nu}] \\ \Pr[\langle j, G, 1\rangle^-_{\nu+1} \mid \langle i, B\rangle^-_{\nu}] & \Pr[\langle j, B, 1\rangle^-_{\nu+1} \mid \langle i, B\rangle^-_{\nu}] \end{pmatrix}, \\
\boldsymbol{S}_{i,j} &= \begin{pmatrix} \Pr[\langle j, G, 0\rangle^-_{\nu+1} \mid \langle i, G\rangle^-_{\nu}] & \Pr[\langle j, B, 0\rangle^-_{\nu+1} \mid \langle i, G\rangle^-_{\nu}] \\ \Pr[\langle j, G, 0\rangle^-_{\nu+1} \mid \langle i, B\rangle^-_{\nu}] & \Pr[\langle j, B, 0\rangle^-_{\nu+1} \mid \langle i, B\rangle^-_{\nu}] \end{pmatrix},
\end{aligned}$$

where $\langle j, s\rangle^-_{\nu}$ and $\langle j, s, \theta\rangle^-_{\nu}$ represent events $\{\widehat{L}^-_{\nu} = j,\ \widehat{S}^-_{\nu} = s\}$ and $\{\widehat{L}^-_{\nu} = j,\ \widehat{S}^-_{\nu} = s, \Theta_{\nu-1} = \theta\}$, respectively. Let $\boldsymbol{R}$ and $\boldsymbol{S}$ denote $2(K+1) \times 2(K+1)$ matrices such that

$$\begin{aligned}
\boldsymbol{R} &= \begin{pmatrix} \boldsymbol{R}_{0,0} & \boldsymbol{R}_{0,1} & \cdots & \boldsymbol{R}_{0,K} \\ \boldsymbol{R}_{1,0} & \boldsymbol{R}_{1,1} & \cdots & \boldsymbol{R}_{1,K} \\ \vdots & \vdots & \ddots & \vdots \\ \boldsymbol{R}_{K,0} & \boldsymbol{R}_{K,1} & \cdots & \boldsymbol{R}_{K,K} \end{pmatrix}, \\
\boldsymbol{S} &= \begin{pmatrix} \boldsymbol{S}_{0,0} & \boldsymbol{S}_{0,1} & \cdots & \boldsymbol{S}_{0,K} \\ \boldsymbol{S}_{1,0} & \boldsymbol{S}_{1,1} & \cdots & \boldsymbol{S}_{1,K} \\ \vdots & \vdots & \ddots & \vdots \\ \boldsymbol{S}_{K,0} & \boldsymbol{S}_{K,1} & \cdots & \boldsymbol{S}_{K,K} \end{pmatrix},
\end{aligned}$$

respectively. Since $\{\Theta_\nu = 1\}$ implies that the number of lost packets in block ν is greater than N,

$$\boldsymbol{R} = \sum_{k=N+1}^{M} \boldsymbol{P}_M^{-+}(k)\boldsymbol{\Gamma}^{+-}, \qquad \boldsymbol{S} = \sum_{k=0}^{N} \boldsymbol{P}_M^{-+}(k)\boldsymbol{\Gamma}^{+-}. \tag{4.9}$$

Further it is easy to see that

$$\begin{aligned}
&\lim_{\nu\to\infty} \mathbb{P}_\gamma[(\Theta_\nu, \Theta_{\nu+1}) = (0,1)] = \boldsymbol{\pi}^- \boldsymbol{S}\boldsymbol{R}\boldsymbol{e}, \\
&\lim_{\nu\to\infty} \mathbb{P}_\gamma[(\Theta_\nu, \Theta_{\nu+1}, \ldots, \Theta_{\nu+n}, \Theta_{\nu+n+1}) = (0,1,\ldots,1,0)] \\
&\qquad\qquad = \boldsymbol{\pi}^- \boldsymbol{S}\boldsymbol{R}^n\boldsymbol{S}\boldsymbol{e}, \qquad n \in \mathbb{N}.
\end{aligned}$$

Thus from (4.7), we obtain

$$P_{\mathrm{BL}}(n) = \frac{\boldsymbol{\pi}^- \boldsymbol{S}\boldsymbol{R}^n\boldsymbol{S}\boldsymbol{e}}{\boldsymbol{\pi}^- \boldsymbol{S}\boldsymbol{R}\boldsymbol{e}}, \qquad n \in \mathbb{N}. \tag{4.10}$$

Similarly we have

$$P_{\mathrm{BS}}(n) = \frac{\boldsymbol{\pi}^- \boldsymbol{R}\boldsymbol{S}^n\boldsymbol{R}\boldsymbol{e}}{\boldsymbol{\pi}^- \boldsymbol{R}\boldsymbol{S}\boldsymbol{e}}, \qquad n \in \mathbb{N}. \tag{4.11}$$

From (4.10) and (4.11), the averages and the variances of the block-loss run length X_{BL} and

the block-success run length $X_{\rm BS}$ are given by

$$\mathrm{E}[X_{\rm BS}] = \frac{\boldsymbol{\pi}^{-}\boldsymbol{R}\boldsymbol{S}(\boldsymbol{I}-\boldsymbol{S})^{-1}\boldsymbol{e}}{\boldsymbol{\pi}^{-}\boldsymbol{R}\boldsymbol{S}\boldsymbol{e}}, \tag{4.12}$$

$$\mathrm{E}[X_{\rm BL}] = \frac{\boldsymbol{\pi}^{-}\boldsymbol{S}\boldsymbol{R}(\boldsymbol{I}-\boldsymbol{R})^{-1}\boldsymbol{e}}{\boldsymbol{\pi}^{-}\boldsymbol{S}\boldsymbol{R}\boldsymbol{e}}, \tag{4.13}$$

$$\mathrm{Var}[X_{\rm BS}] = \frac{\boldsymbol{\pi}^{-}\boldsymbol{R}\boldsymbol{S}(\boldsymbol{I}-\boldsymbol{S})^{-2}(\boldsymbol{I}+\boldsymbol{S})\boldsymbol{e}}{\boldsymbol{\pi}^{-}\boldsymbol{R}\boldsymbol{S}\boldsymbol{e}} - \left(\mathrm{E}[X_{\rm BS}]\right)^2, \tag{4.14}$$

$$\mathrm{Var}[X_{\rm BL}] = \frac{\boldsymbol{\pi}^{-}\boldsymbol{S}\boldsymbol{R}(\boldsymbol{I}-\boldsymbol{R})^{-2}(\boldsymbol{I}+\boldsymbol{R})\boldsymbol{e}}{\boldsymbol{\pi}^{-}\boldsymbol{S}\boldsymbol{R}\boldsymbol{e}} - \left(\mathrm{E}[X_{\rm BL}]\right)^2, \tag{4.15}$$

respectively.

In what follows, we discuss the computational complexity of the performance measures $\mathrm{E}[X_{\rm BS}]$, $\mathrm{E}[X_{\rm BL}]$, $\mathrm{Var}[X_{\rm BS}]$ and $\mathrm{Var}[X_{\rm BL}]$. According to (4.12)–(4.15), the computation of these performance measures requires the vector $\boldsymbol{\pi}^{-}$ and two matrices $\boldsymbol{R}$ and $\boldsymbol{S}$.

We first consider the computational complexity of $\boldsymbol{\pi}^{-}$. Recall here that $\boldsymbol{\pi}^{-}$ is the stationary probability vector of the $2(K+1)\times 2(K+1)$ stochastic matrix $\boldsymbol{\Pi}^{--} = \boldsymbol{\Lambda}^{-+}\boldsymbol{\Gamma}^{+-}$ (see (4.1)). Applying the uniformization technique (see, e.g., pp. 57–58 in [14]) to (4.3), we can calculate $\boldsymbol{\Gamma}^{+-}$ as follows:

$$\boldsymbol{\Gamma}^{+-} \approx \sum_{n=0}^{H} \mathrm{e}^{-\theta x}\frac{(\theta x)^n}{n!}\mathrm{d}G(x)[\boldsymbol{I}+\theta^{-1}\boldsymbol{Q}]^n,$$

where H is a sufficiently large positive integer and θ is the maximum absolute value of the diagonal elements of $\boldsymbol{Q}$. Thus the computational complexity of $\boldsymbol{\Gamma}^{+-}$ is expressed as $O(H\{2(K+1)\}^3) = O(HK^3)$. Further, given $\boldsymbol{\Gamma}^{+-}$, we can calculate $\boldsymbol{\pi}^{-}$ by the LU-decomposition, which takes $O(\{2(K+1)\}^3) = O(K^3)$ complexity. Consequently, the computational complexity of $\boldsymbol{\pi}^{-}$ is $O(HK^3)$.

Next we consider the computation of $\boldsymbol{R}$ and $\boldsymbol{S}$ given in (4.9), which requires the $\boldsymbol{P}_M(k)$'s $(k=0,1,\ldots,M)$. In computing these matrices by the recursion (4.5) and (4.6), we have to perform $(M-1)(2M+1)$ products of $2(K+1)\times 2(K+1)$ matrices. Therefore the computational complexity of $\boldsymbol{R}$ and $\boldsymbol{S}$ is $O((M-1)(2M+1)\{2(K+1)\}^3) = O(M^2K^3)$.

As a result, the total computational complexity of the four performance measures is $O((H+M^2)K^3)$.

5. Numerical Examples

In this section, we consider video streaming as main traffic and evaluate block-loss and block-success runs using the results derived in the previous section. It is assumed that bit rate and frame rate of the video stream are 4 Mb/s and 30 frame/s, respectively. A frame of the video corresponds to a block, which consists of $D=34$ data packets. The size of a packet is 500 bytes. Inter-arrival times of packets from main traffic are constant. Note that when N redundant packets are added to original D data packets, the resulting arrival rate of main traffic is $(D+N)/D$ times larger than the original one. An output transmission rate of the wireless base station in Good (resp. Bad) state is 40 Mb/s (resp. 4 Mb/s), and the corresponding service rate of a 500 byte-packet, μ_G (resp. μ_B), is 1.0×10^4 (resp. $\mu_G = 1.0\times 10^3$). Mean Good-state and Bad-state periods are 95 ms and 5 ms, respectively.

We conducted trace-driven simulation experiments to validate the analytical model. Our simulation program was developed with C#, and the trace data of the NLANR repository

Table 1: Trace data information used for simulation experiments

Name	Original filename	Date/Capt. on
Leipzig-II	20030221-121359-0.g2	February 2003/OC3

Table 2: Basic parameters of numerical calculation

Parameter	Value
Packet size (bytes)	500
Number of data packets in a block D	34
Number of redundant packets in a block N	0, 1, 3
Service rate of a packet in Good state μ_G	1.0×10^4
Service rate of a packet in Bad state μ_B	1.0×10^3
Mean time in Good state $1/\alpha$ (ms)	95
Mean time in Bad state $1/\beta$ (ms)	5
Arrival rate of background traffic λ	6.23×10^3
System capacity K	10, 100

[19] was used for inter-arrival times of packets in background traffic. Table 1 shows the detail of the trace. Figure 3 illustrates the volume of the trace data for 200 seconds we used. Figure 4 shows the histogram of inter-arrival times of the trace data and probability distribution function of the exponential distribution whose average is equal to the trace data. When the packet size is 500 bytes, the average volume of the trace is 24.9 Mb/s, and the corresponding arrival rate of background traffic λ is 6.23×10^3. The variance of the inter-arrival times for the trace is 3.01×10^{-2}, while that for the exponential distribution is 2.57×10^{-2}, i.e., the variance of the trace is larger than that of Poisson process. Table 2 shows basic parameters of our numerical calculation.

5.1. Impact of system capacity

In this subsection, we investigate how the system capacity K affects the mean block-loss and block-success run lengths. Figure 5 (resp. Figure 6) illustrates the mean block-loss run length $\mathrm{E}[X_{\mathrm{BL}}]$ (resp. the mean block-success run length $\mathrm{E}[X_{\mathrm{BS}}]$) against the system capacity for the number of redundant packets $N = 0, 1$, and 3. Analytical results are plotted with lines, while simulation results are shown by dots with 95% confidence intervals. In Figure 5, we observe the quantitative difference between analytical and simulation results. This is because the statistical nature of the trace data for simulation is different from the Poisson process assumed in analysis. However, both analytical and simulation results decrease monotonically as the system capacity K increases. We observe from Figure 6 that both analytical and simulation results increase monotonically as the system capacity K increases. These results suggests that the analysis is efficient in a qualitative sense to investigate the behavior of consecutive block-loss and block-success events.

A remarkable point here is that FEC with high redundancy makes $\mathrm{E}[X_{\mathrm{BL}}]$ significantly small. This implies that consecutive block loss can be effectively prevented with FEC even when the system capacity is small.

Figure 7 (resp. Figure 8) represents the variance of the block-loss run length X_{BL}

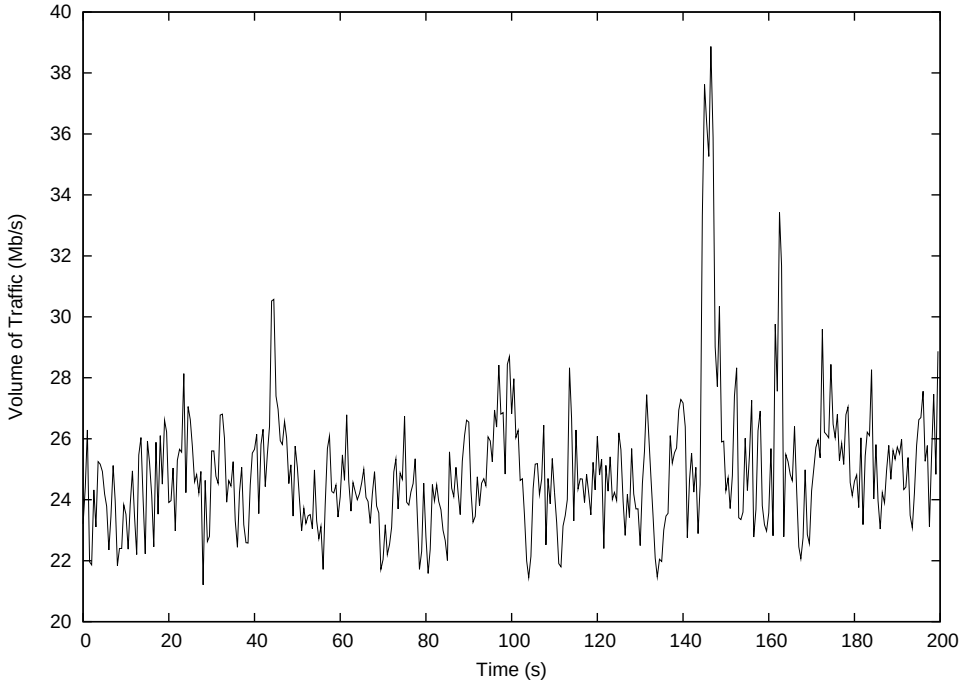

Figure 3: Volume of trace data vs. time

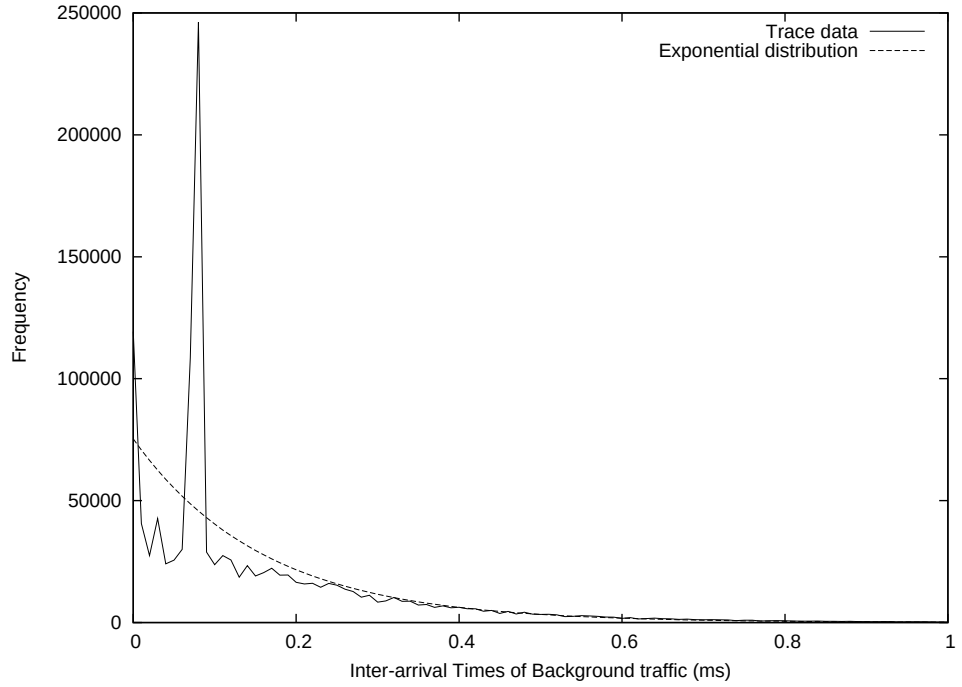

Figure 4: Histogram of trace data and corresponding probability density function of exponential distribution

(resp. the variance of the block-success run length X_{BS}) against K in cases of $N = 0, 1$, and 3. In Figure 7, the variance of the block-loss run length decreases monotonically with the increase in K for each N. In each K, the variance of the block-loss run length for $N = 0$ is the largest, while that for $N = 3$ is the smallest. Note that the variance of the block-loss run length is small even for $K = 10$ and $N = 0$. This implies that the block-loss run length

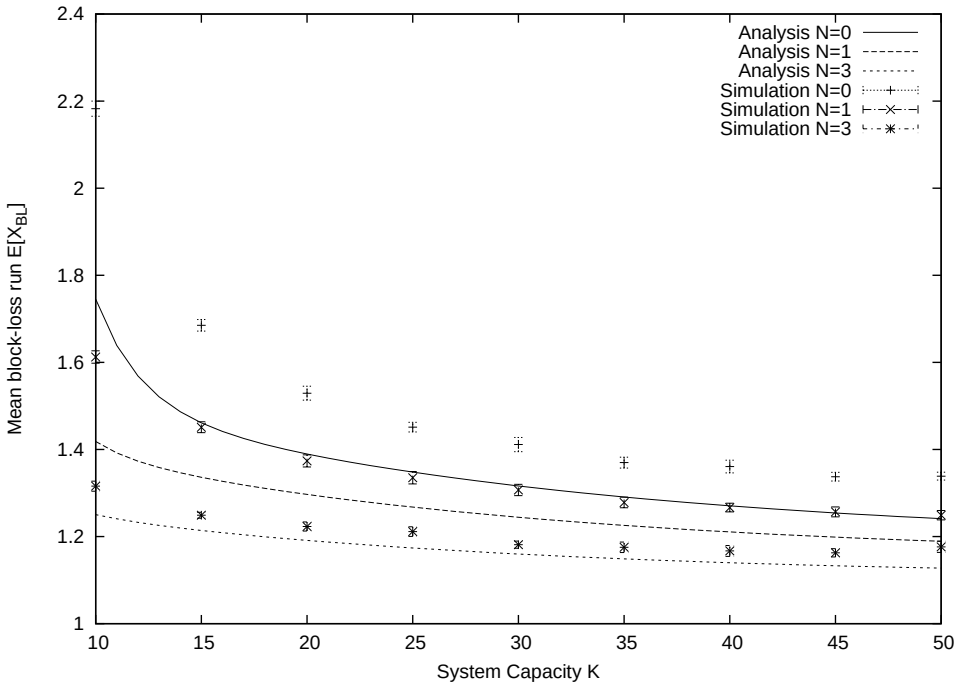

Figure 5: Mean block-loss run length $\mathrm{E}[X_{\mathrm{BL}}]$ vs. system capacity K

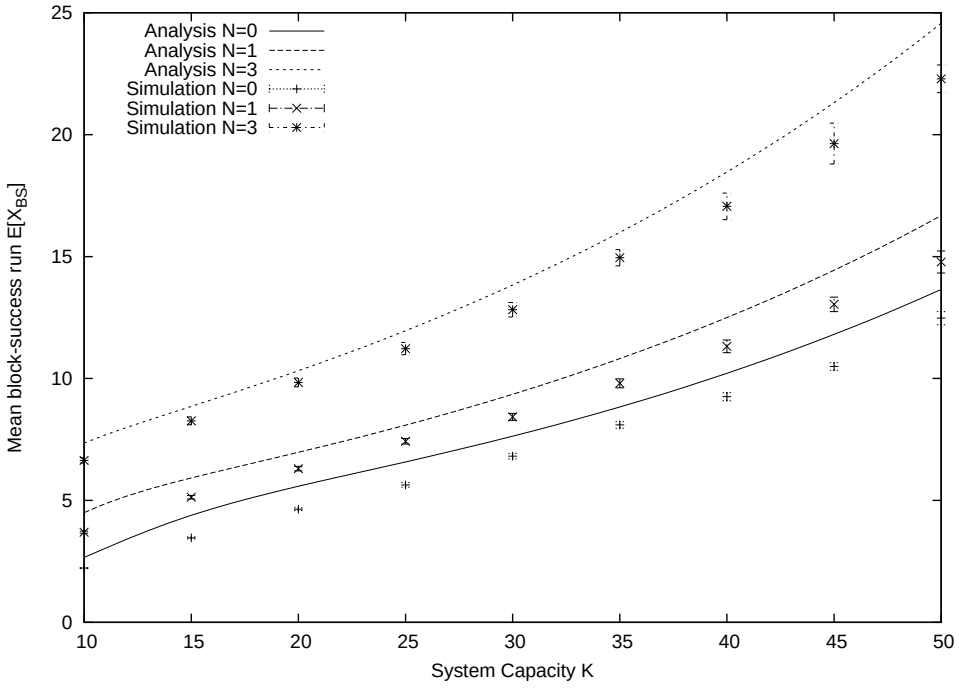

Figure 6: Mean block-success run length $\mathrm{E}[X_{\mathrm{BS}}]$ vs. system capacity K

is well prevented by the system capacity, rather than FEC.

In Figure 8, on the other hand, the variance of the block-success run length grows with the increase in K. A remarkable point here is that the variance for $N = 3$ significantly increases against K. From both Figs. 7 and 8, we can claim that the block-loss run length is significantly improved by enhancing the system capacity rather than increasing the FEC redundancy, and that the variation of the block-success run length is greatly affected by the

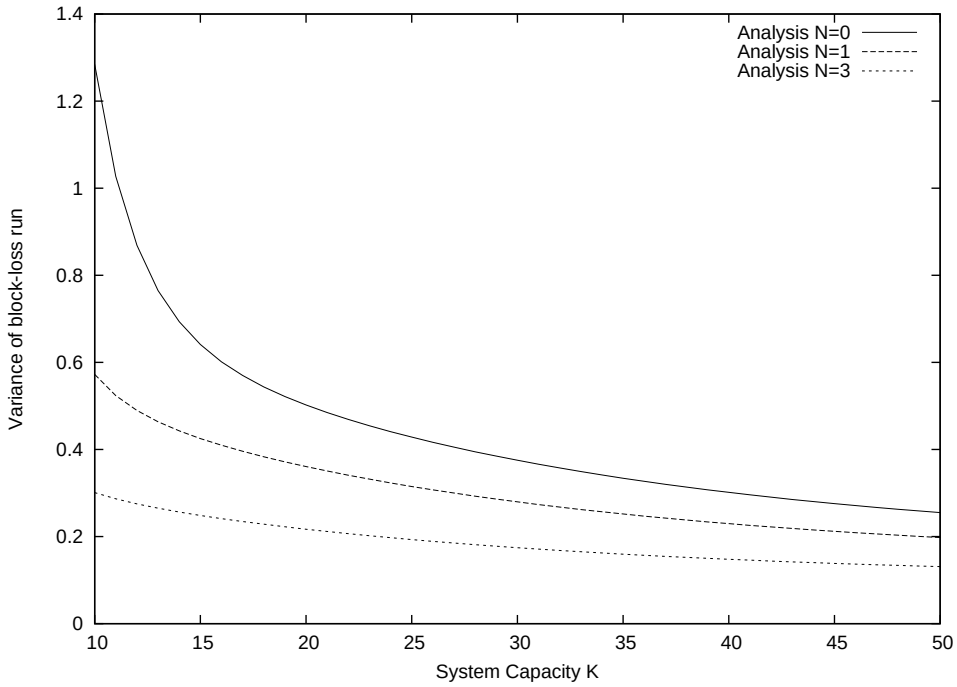

Figure 7: Variance of block-loss run length $\mathrm{Var}[X_{\mathrm{BL}}]$ vs. system capacity K

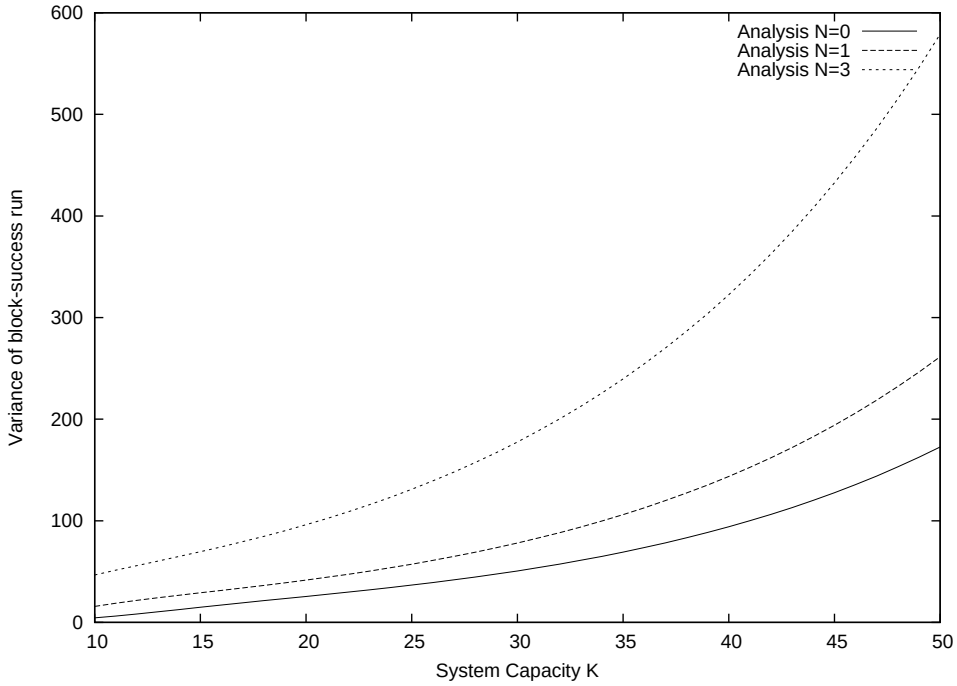

Figure 8: Variance of block-success run length $\mathrm{Var}[X_{\mathrm{BS}}]$ vs. system capacity K

FEC redundancy.

5.2. Impact of background traffic

In this subsection, we investigate how the mean block-loss and block-success runs are affected by the volume of background traffic. Figs. 9 and 10 show the mean block-loss run length $\mathrm{E}[X_{\mathrm{BL}}]$ and block-success run length $\mathrm{E}[X_{\mathrm{BS}}]$ against the volume of background traffic,

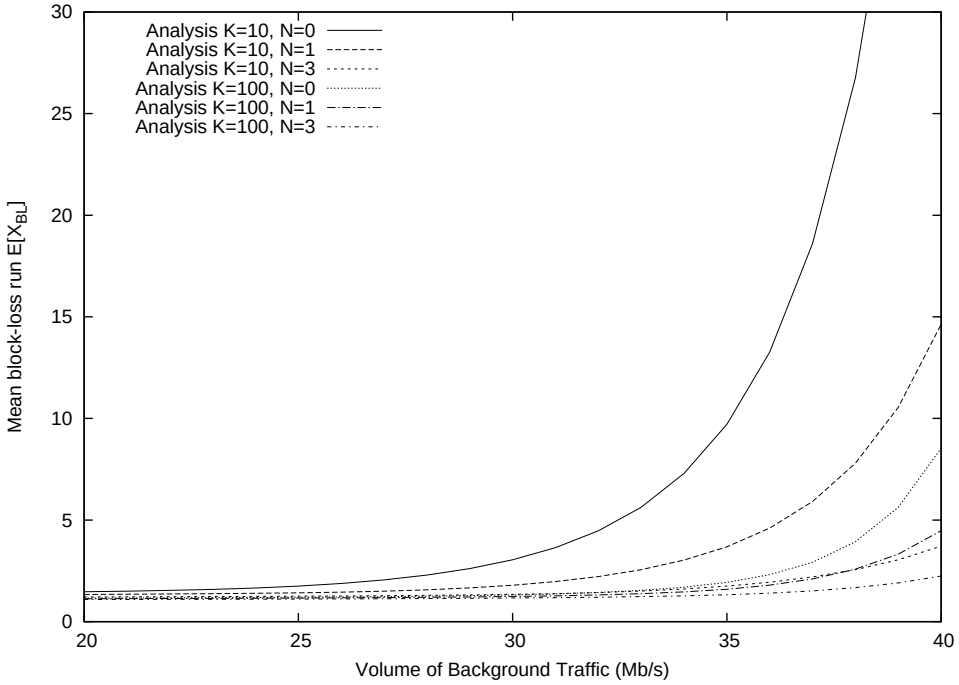

Figure 9: Mean block-loss run length $\mathrm{E}[X_{\mathrm{BL}}]$ vs. background traffic

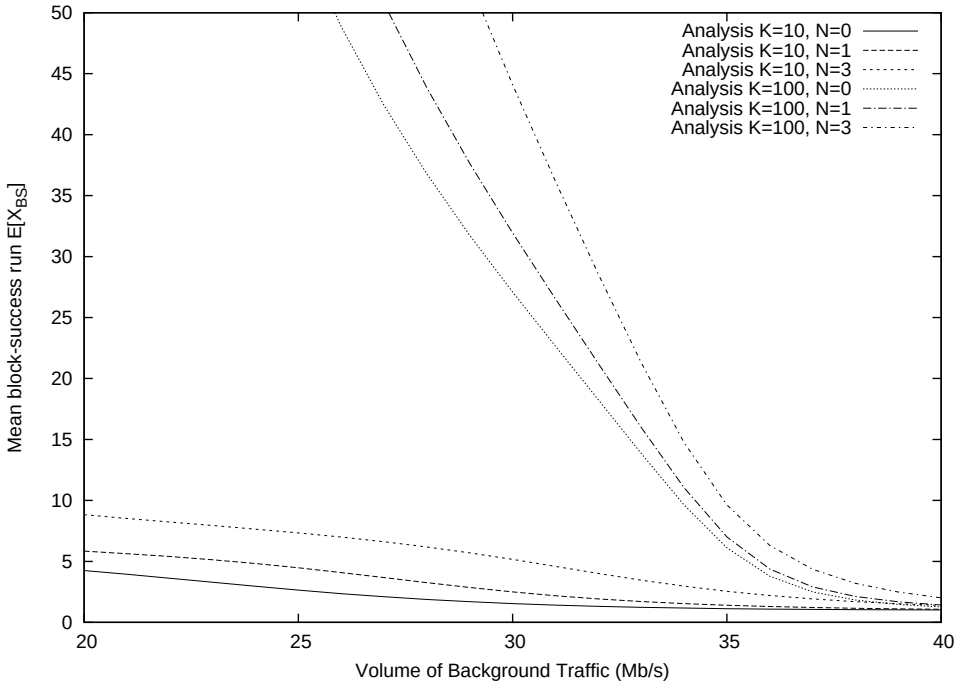

Figure 10: Mean block-success run length $\mathrm{E}[X_{\mathrm{BS}}]$ vs. background traffic

respectively. When the volume of background is γ Mb/s, the corresponding packet arrival rate λ is equal to $\gamma \times 250$ packet/s. Note that only analytical results are shown in both graphs because the trace data only supports 24.9 Mb/s background traffic case.

It is observed from Figure 9 that $\mathrm{E}[X_{\mathrm{BL}}]$ increases as the volume of background traffic increases. It is remarkable that a gradient for high redundancy is smaller than that for low ones. This implies that FEC is effective even when background traffic is large.

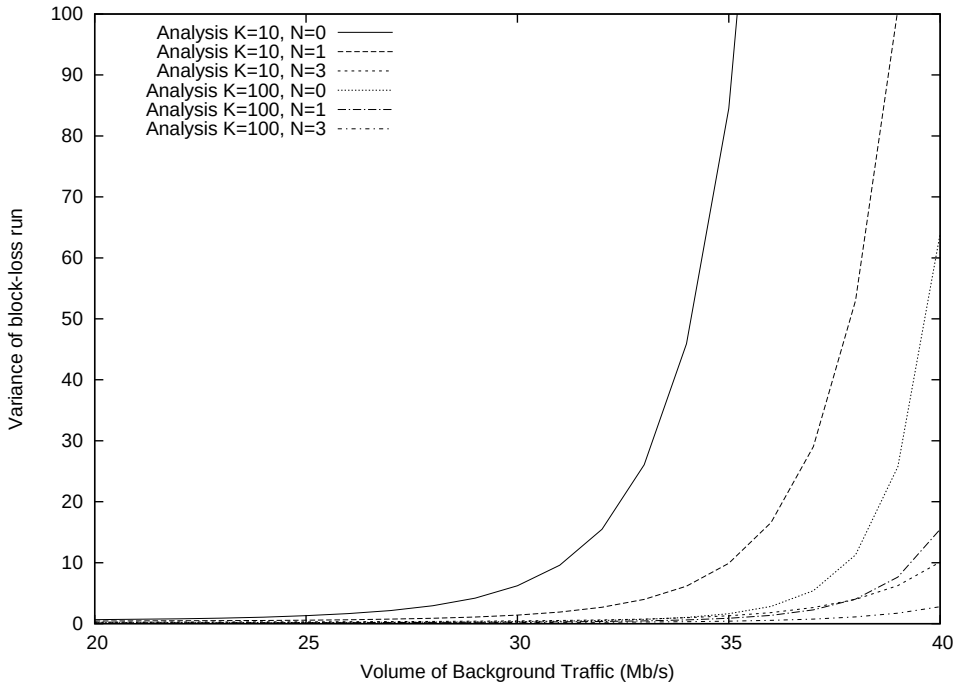

Figure 11: Variance of block-loss run length $\mathrm{Var}[X_{\mathrm{BL}}]$ vs. background traffic

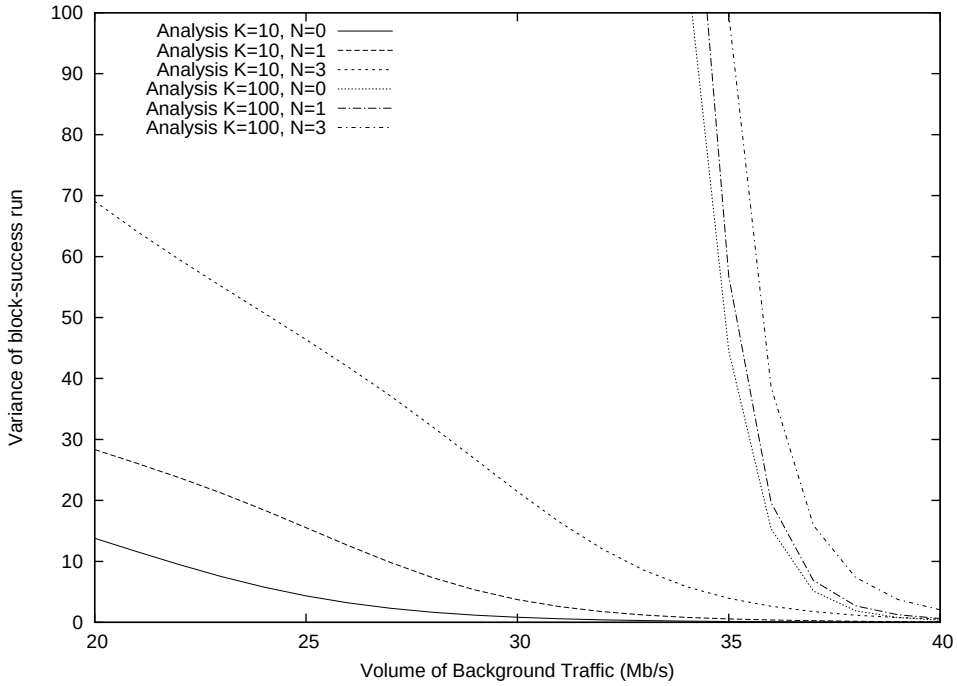

Figure 12: Variance of block-success run length $\mathrm{Var}[X_{\mathrm{BS}}]$ vs. background traffic

In Figure 10, we observe that $\mathrm{E}[X_{\mathrm{BS}}]$ decreases monotonically as the volume of background traffic increases. In particular, all the three cases for $K = 100$ show a rapid decrease. This implies that when the volume of background traffic is small, $\mathrm{E}[X_{\mathrm{BS}}]$ is dominantly affected by the system capacity K.

Figure 11 (resp. Figure 12) shows the variance of the block-loss run length X_{BL} (resp. the variance of the block-success run length X_{BS}) against the volume of background traffic in

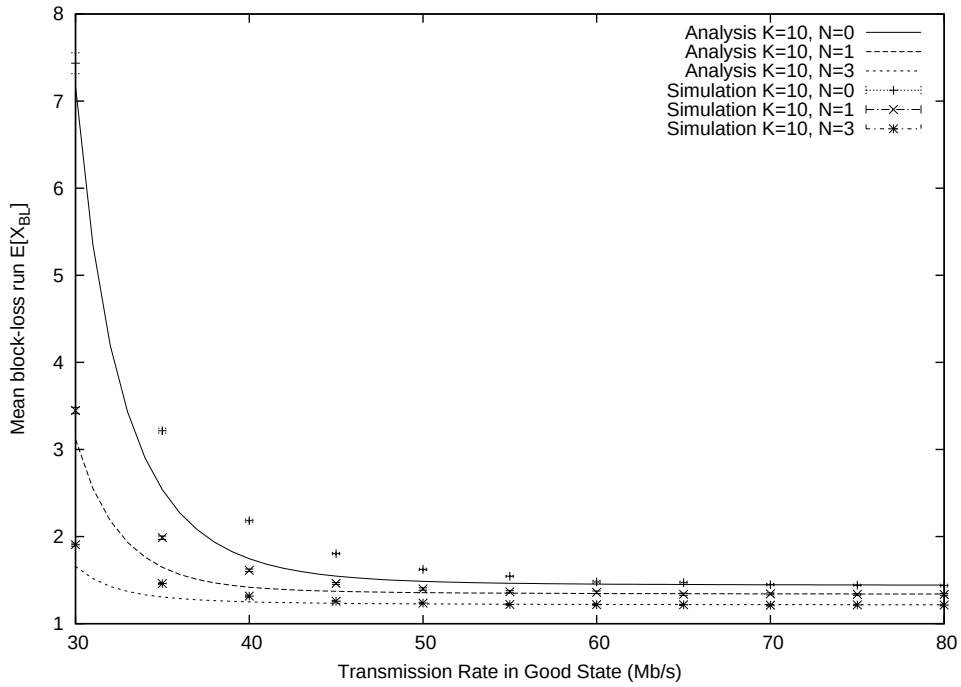

Figure 13: Mean block-loss run length $\mathrm{E}[X_{\mathrm{BL}}]$ vs. transmission rate in Good state

cases of $N = 0, 1$, and 3. In both figures, we calculated the variances for $K = 10$ and 100. In Figure 11, the variance of the block-loss run length for each case increases exponentially with the increase in the volume of background traffic. It is also observed from this figure that the variance of the block-loss run length is significantly decreased by FEC.

In Figure 12, on the other hand, the variance of the block-success run length decreases when the volume of background traffic is growing. In particular, when $K = 100$, the variance of the block-success run length suddenly decreases around 35 Mb/s background traffic. Figs. 11 and 12 suggest that the block-success run length is likely to shorten under heavy loaded condition, resulting in frequent block-loss. In this situation, FEC is significantly effective to prevent a long block-loss run length.

5.3. Impact of transmission rate in Good state

In this subsection, we investigate how the transmission rate in Good state affects the mean block-loss and block-success runs. Figure 13 (resp. Figure 14) shows the mean block-loss run length $\mathrm{E}[X_{\mathrm{BL}}]$ (resp. the mean block-success run length $\mathrm{E}[X_{\mathrm{BS}}]$) against the transmission rate in Good state for $K = 10$. When the transmission rate in Good state is δ Mb/s, the corresponding service rate of a packet in Good state μ_G is equal to $\delta \times 250$ packet/s.

We observe from Figure 13 that $\mathrm{E}[X_{\mathrm{BL}}]$ decreases and then remains constant as the transmission rate in Good state increases. On the contrary, it is observed from Figure 14 that $\mathrm{E}[X_{\mathrm{BS}}]$ increases and then converges to a certain value with the increase in the transmission rate in Good state. This is because for a large transmission rate in Good state, a packet-loss event occurs in Bad state, rather than in Good state. Therefore, mean block-loss and block-success run lengths stay constant when the transmission rate in Good state is large.

Note that in both the figures, analytical results show a good agreement with simulation ones when the packet transmission rate in Good state increases. This suggests that the analytical model is useful for estimating block-loss and block-success run lengths for a high-

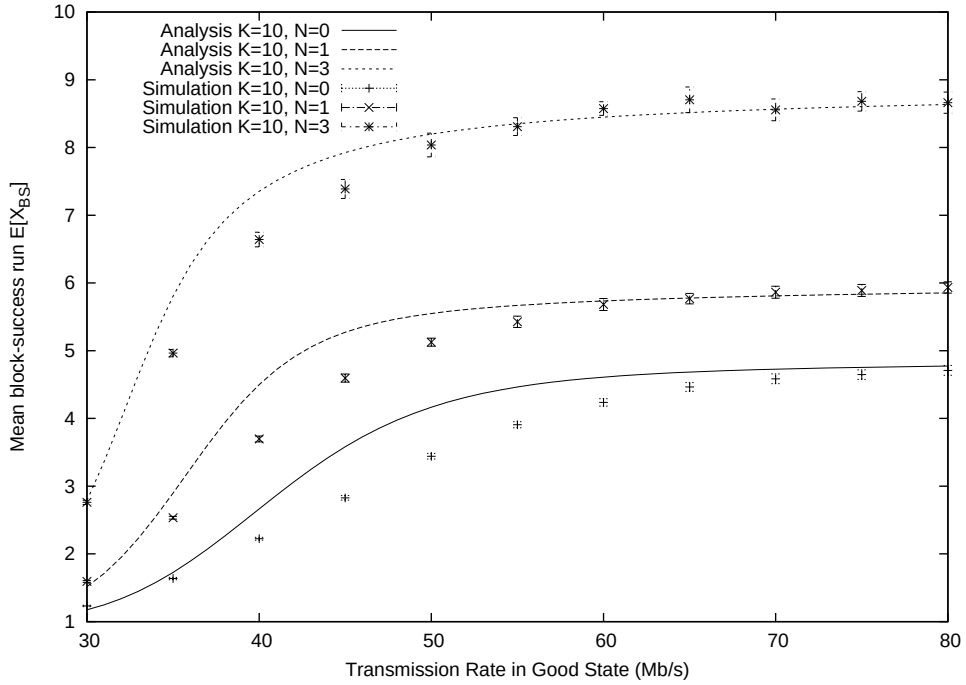

Figure 14: Mean block-success run length $\mathrm{E}[X_{\mathrm{BS}}]$ vs. transmission rate in Good state

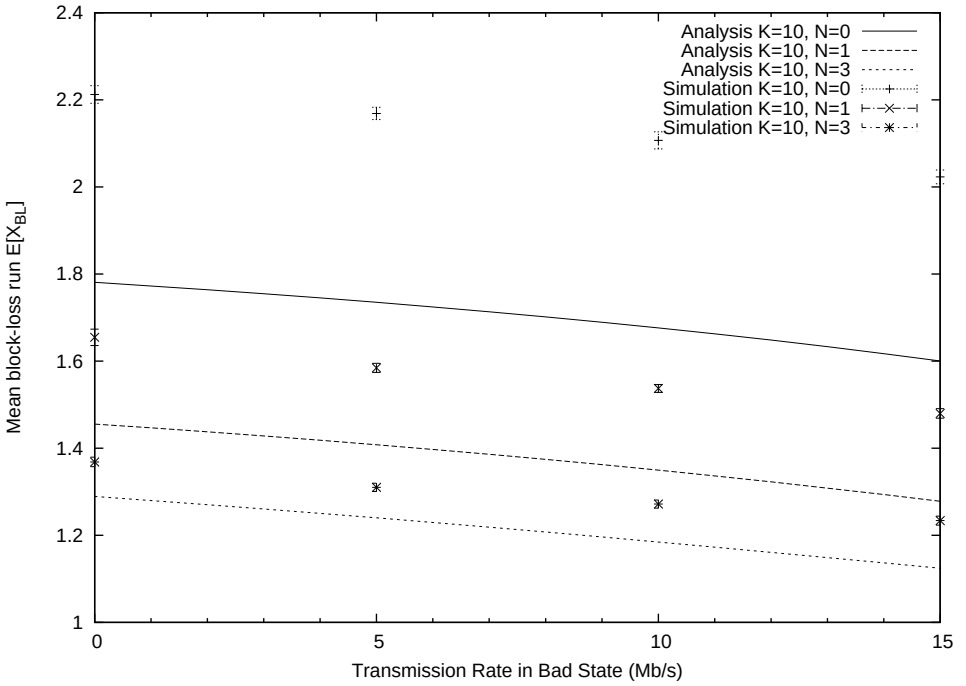

Figure 15: Mean block-loss run length $\mathrm{E}[X_{\mathrm{BL}}]$ vs. transmission rate in Bad state

speed wireless network environment.

5.4. Impact of transmission rate in Bad state

In this subsection, we investigate how the mean block-loss and block-success runs are affected by the transmission rate in Bad state. Figure 15 (resp. Figure 16) illustrates the mean block-loss run length $\mathrm{E}[X_{\mathrm{BL}}]$ (resp. the mean block-success run length $\mathrm{E}[X_{\mathrm{BS}}]$) against the

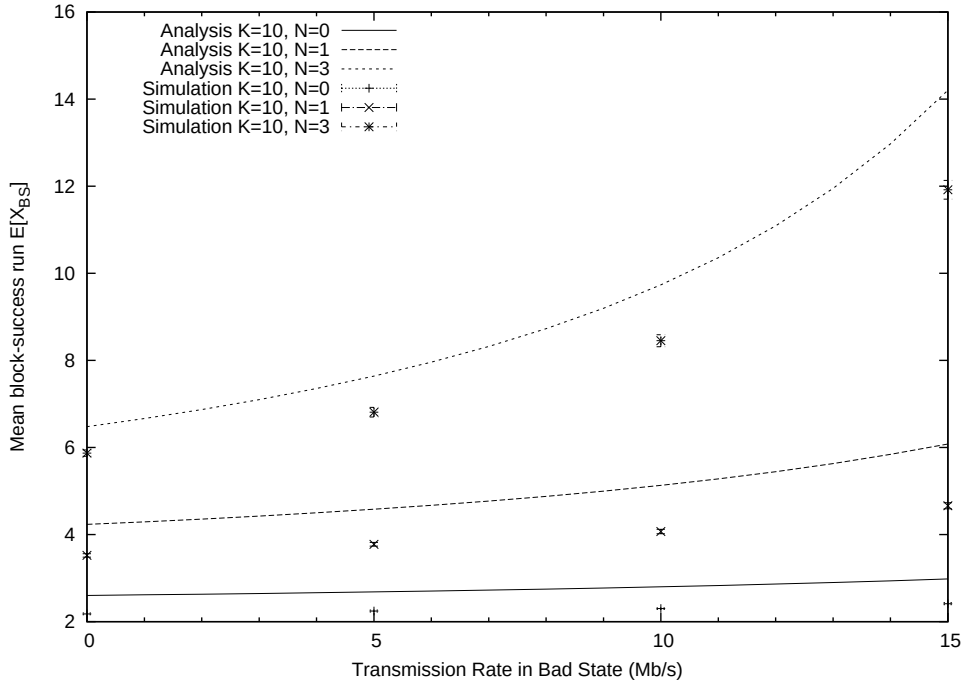

Figure 16: Mean block-success run length $\mathrm{E}[X_{\mathrm{BS}}]$ vs. transmission rate in Bad state

transmission rate in Bad state for $K = 10$. When the transmission rate in Bad state is ε Mb/s, the corresponding service rate of a packet in Bad state μ_B is equal to $\varepsilon \times 250$ packet/s.

In Figure 15, we observe that $\mathrm{E}[X_{\mathrm{BL}}]$ decreases monotonically as the transmission rate in Bad state increases, as expected. Note that the slight decrease for each N is due to the small sojourn time in Bad state. (Remind that the mean Bad-state period is 5 ms, while the mean Good-state period is 95 ms.)

It is observed from Figure 16 that $\mathrm{E}[X_{\mathrm{BS}}]$ increases monotonically as the transmission rate in Bad state increases. It is remarkable that for any transmission rate in Bad state, $\mathrm{E}[X_{\mathrm{BS}}]$ with a large N is greater than that with a small N. This implies that the transmission rate in Bad state is dominant in the case of large N.

5.5. Impact of Bad-state period

Finally, we investigate how the mean block-loss and block-success runs are affected by the mean Bad-state period. Figs. 17 and 18 show the mean block-loss run length $\mathrm{E}[X_{\mathrm{BL}}]$ and block-success run length $\mathrm{E}[X_{\mathrm{BS}}]$ against the mean time in Bad state $1/\beta$ for $K = 10$, respectively.

We observe from Figure 17 that $\mathrm{E}[X_{\mathrm{BL}}]$ increases linearly as the mean time in Bad state increases. This implies that the Bad-state period affects $\mathrm{E}[X_{\mathrm{BL}}]$ dominantly. In Figure 18, $\mathrm{E}[X_{\mathrm{BS}}]$ decreases monotonically and then remains constant as the the mean time in Bad state increases. A remarkable point here is that when the mean time in Bad state is small, $\mathrm{E}[X_{\mathrm{BS}}]$ is significantly different among the cases $N = 0, 1$, and 3. This suggests that when the wireless link guarantees a good quality of data transmission, FEC is significantly effective in increasing the block-success run length.

5.6. Discussion on QoS guarantee

One of simple frame-error recovery schemes is frame repetition with which a lost frame is replaced by the previous reconstructed frame. It is reported in [22] that for 20 frame/s video, four same frames consecutively displayed are not perceptually acceptable for end

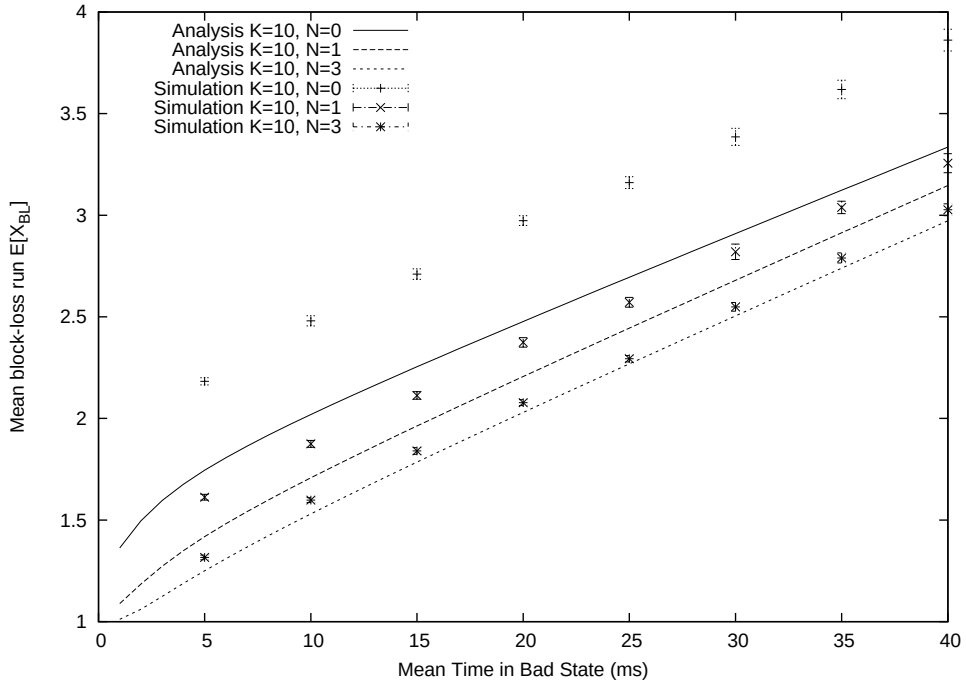

Figure 17: Mean block-loss run length $\mathrm{E}[X_{\mathrm{BL}}]$ vs. mean time in Bad state

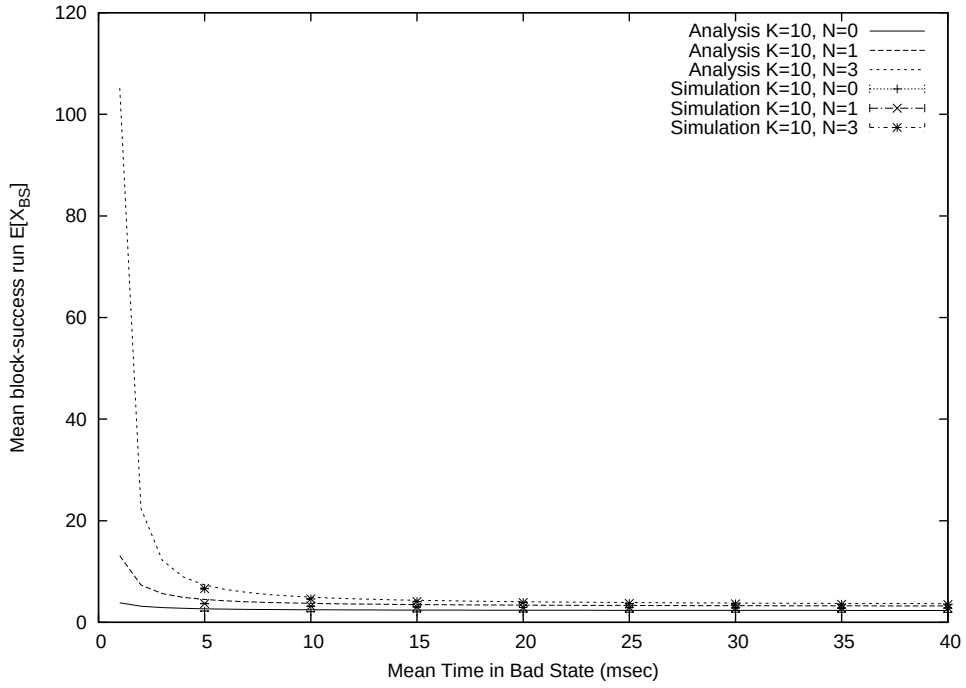

Figure 18: Mean block-success run length $\mathrm{E}[X_{\mathrm{BS}}]$ vs. mean time in Bad state

users. In our numerical experiments, the frame rate is 30 frame/s, and hence we consider the following criteria for QoS guarantee. The maximum number of the mean block-loss run length is five, and the minimum number of the mean block-success run length is 25.

From Figure 5, we observe that the mean block-loss run length is smaller than five for $10 \leq K \leq 50$, while the mean block-success run length is smaller than 25 for all N's in Figure 6. In Figure 9, when $K = 100$, the mean block-loss run length can be kept under five

for a wide range of the volume of background traffic. On the other hand, it is observed from Figure 10 that for $K = 100$, even $N = 3$ FEC redundancy cannot satisfy the QoS criterion of the block-success run length when the volume of background traffic is greater than 33 Mb/s. Furthermore, Figure 15 shows that when $K = 10$, the mean block-loss run length can be kept smaller than five until the mean duration time in Bad state reaches 40 ms. In Figure 16, however, the mean block-success run length for $N = 3$ becomes unacceptable when the mean duration time in Bad state is greater than 2 ms.

These results imply that the block-loss run length can be well controlled by the system capacity or by FEC. On the other hand, it is difficult to improve the block-success run length by the system capacity and FEC. Note that the above discussion assumes that the frame-error recovery scheme is frame repetition. In terms of the other error error concealment schemes, further investigation is needed.

6. Conclusion

In this paper, we considered the characterization of block-loss and block-success run events for video streaming services. We modeled the wireless base station as a single-server finite queueing system with two input processes and Markovian service process, analyzing the block-loss and block-success run distributions. It was assumed in our model that the packet inter-arrival times of video traffic using FEC is independent and identically distributed. This enables us to analyze the system with a various type of the arrival process for video traffic. It was shown from numerical examples that the analytical model is useful in a qualitative sense for investigating the behavior of consecutive block-loss and block-success events. Numerical examples also showed that block-loss run and block-success run are significantly affected by the volume of background traffic. Even when the traffic intensity is high, FEC is effective in decreasing the block-loss run length. On the other hand, when the traffic intensity is low, the block-success run is significantly affected by the system capacity. In terms of application-level QoS, consecutive block loss makes loss concealment difficult. Therefore, it is worth noting that FEC is more effective in decreasing the block-loss run length than in enhancing the system capacity.

In the analytical model, we assumed that packet transmission times in both Good and Bad states follow exponential distributions. Note that the exponential distribution is a special case of the gamma distribution, with which empirical distributions for packet transmission times over wireless links are well fitted [2]. Therefore, further measurement study is needed for modeling the packet transmission time distribution.

References

[1] I. F. Akyildiz, X. Wang, and W. Wang: Wireless mesh networks: a survey. *Computer Networks*, **47** (2005), 445–487.

[2] N. A. Ali, E. Ekram, A. Eljasmy, and K. Shuaib: Measured delay distribution in a wireless mesh network test-bed. *Proceedings of ACS/IEEE International Conference on Computer Systems and Applications*, (2008), 236–240.

[3] E. Altman and A. Jean-Marie: Loss probabilities for messages with redundant packets feeding a finite buffer. *IEEE Journal on Selected Areas in Communications*, **16** (1998), 778–787.

[4] D. Bertsekas and R. Gallager: *Data Networks 2nd edition* (Prentice Hall, 1992).

[5] H. M. Chaskar, T. V. Lakshman, and U. Madhow: TCP over wireless with link level

error control: analysis and design methodology. *IEEE/ACM Transactions on Networking*, **7** (1999), 605–615.

[6] I. Cidon, A. Khamisy, and M. Sidi: Analysis of packet loss processes in high-speed networks. *IEEE Transactions on Information Theory*, **39** (1993), 98–108.

[7] G. Dán, V. Fodor, and G. Karlsson: On the effects of the packet size distribution on the packet loss process. *Telecommunication Systems*, **32** (2006), 31–53.

[8] G. Dán, V. Fodor, and G. Karlsson: On the effects of the packet size distribution on FEC performance. *Computer Networks*, **50** (2006), 1104–1129.

[9] P. E. Green: Fiber to the home: the next big broadband thing. *IEEE Communications Magazine*, **42** (2004), 100–106.

[10] O. A. Hellal, E. Altman, A. Jean-Marie, and I. A. Kurkova: On loss probabilities in presence of redundant packets and several traffic sources. *Performance Evaluation*, **36–37** (1999), 485–518.

[11] W. Jiang and H. Schulzrinne: Modeling of packet loss and delay and their effect on real-time multimedia service quality. *Proceedings of NOSSDAV 2000*, (2000).

[12] K. Kato, H. Masuyama, S. Kasahara, and Y. Takahashi: Analysis of consecutive block-loss for streaming services. *Proceedings of IEEE ICC 2010*, (2010).

[13] K. Kawahara, K. Kumazoe, T. Takine, and Y. Oie: Forward error correction in ATM networks: an analysis of cell loss distribution in a block. *Proceedings of IEEE INFOCOM '94*, **3** (1994), 1150–1159.

[14] G. Latouche and V. Ramaswami: *Introduction to Matrix Analytic Methods in Stochastic Modeling* (ASA–SIAM, Philadelphia, PA, 1999).

[15] D. Marpe, T. Wiegand and G. J. Sullivan: The H.264/MPEG4 advanced video coding standard and its applications. *IEEE Communications Magazine*, **44** (2006), 134–143.

[16] I. Moccagatta, S. Soudagar, J. Liang and H. Chen: Error-resilient coding in JPEG-2000 and MPEG-4. *IEEE Journal on Selected Areas in Communications*, **18** (2000), 899–914.

[17] S. Muraoka, H. Masuyama, S. Kasahara, and Y. Takahashi: Performance analysis of FEC recovery using finite-buffer queueing system with general renewal and Poisson inputs. *Managing Traffic Performance in Converged Networks (Proceedings of the 20th International Teletraffic Congress - ITC20)*, LNCS4516, Springer-Verlag (2007), 707–718.

[18] S. Muraoka, H. Masuyama, S. Kasahara, and Y. Takahashi: FEC recovery performance for video streaming services over wired-wireless networks. *Performance Evaluation*, **66** (2009), 327–342.

[19] Passive measurement and analysis (PMA). Available: `http://pma.nlar.net/Special/leip2.html`

[20] J. D. Salehi, Z.-L. Zhang, J. Kurose, and D. Towsley: Supporting stored video: Reducing rate variability and end-to-end resource requirements through optimal smoothing. *IEEE/ACM Transactions on Networking*, **6** (1998), 397–410.

[21] N. Shacham and P. E. Mckenney: Packet recovery in high-speed networks using coding and buffer management *Proceedings of IEEE INFOCOM '90*, **1** (1990), 124–131.

[22] J. Tan and N. B. Shroff: Transition from heavy to light tails in retransmission durations. *Proceedings of IEEE INFOCOM 2010*, (2010), 1–9.

[23] A. S. Tanenbaum: *Computer Networks 4th edition* (Prentice Hall, 2002).

[24] M. Yajnik, S. Moon, J. Kurose, and D. Towsley: Measurement and modelling of the temporal dependence in packet loss. *Proceedings of IEEE INFOCOM '99*, **1** (1999), 345–352.

Shoji Kasahara
Graduate School of Information Science
Nara Institute of Science and Technology
8916-5 Takayama, Ikoma
Nara 630-0192, Japan
E-mail: kasahara@ieee.org